



Geometric error sensitivity analysis for a 6-axis welding equipment based on Lie theory

Weihua Fang^{1,2} · Xincheng Tian^{1,2}

Received: 12 June 2020 / Accepted: 15 December 2020 / Published online: 31 January 2021
© The Author(s), under exclusive licence to Springer-Verlag London Ltd. part of Springer Nature 2021

Abstract

The influence of geometric errors on the accuracy of machine tools tends to attract more attention to the increasing demand for high-precision machining. In this paper, geometric error modeling and sensitivity analysis are employed to quantify the importance of geometric error for a new efficient and automatic 6-axis welding equipment. The geometric error model of the 6-axis welding equipment with 36 geometric error components is established based on Lie theory. Based on the geometric error model, the new sensitivity analysis method, in which the deviation of the welding torch pose is treated as a distance metric in $SE(3)$, is proposed to evaluate the influences of geometric errors on the accuracy of the welding torch. And the sensitivity coefficient of each geometric error is derived by considering the basic value of geometric errors. Numerical simulations of a typical welding trajectory for intersecting pipes are conducted to analyze the sensitivity of geometric errors by the new method. The simulation results verified the validity of the sensitivity analysis method and the dominant geometric errors affecting the accuracy of the welding equipment were identified. Compared with the previous sensitivity analysis method, the proposed sensitivity analysis method considers the orientation error and position error of the welding torch simultaneously, which is more convenient and effective, and can also be applied in precision design and geometric error compensation of machine tools.

Keywords Geometric error model · Welding equipment · Sensitivity analysis · Lie theory

1 Introduction

Intersecting pipes welding widely exists in pipeline engineering, steel structure, valve manufacturing, pressure vessel manufacturing, etc. With the development of manufacturing, the industry focuses on the dimensional accuracy and surface finish for improved functioning of the machined parts. The requirement of welding accuracy for welding equipment is increasing. Up to the present, the existing strategies to improve the accuracy of machine tools can be divided into two categories: precision design and error compensation [1]. The strategy of precision design is to improve the precision of components at the design stage of a machine tool. However, the strategy of error compensation tries to

improve the machining accuracy by software or assistant mechanisms without changing the machine tool structure. Compared with error compensation, the cost and degree of difficulty are increasing rapidly with the improvement of machining accuracy by precision design, and the range of application is limited for existing machine tools, though, regardless of which approach is employed to improve the accuracy of a machine tool, geometric error modeling and identifying vital error components are essential steps to do first.

The geometric error sources of machine tools can be mainly classified into four parts: kinematic errors, thermo-mechanical errors, forces, and control errors [2]. As the geometric errors existing in machine tools are inevitable, plenty of researchers focused on geometric error modeling and error analysis. Lin and Shen [3] proposed the matrix summation approach to establish the error model of the five-axis machine tool and broke down the kinematics equation into six components, which decreases the amount of computation and makes the five-axis kinematics model manageable and understandable. Fu et al. [4] established a geometric error model of a multi-axis machine tool based

✉ Xincheng Tian
txch@sdu.edu.cn

¹ Center for Robotics, School of Control Science and Engineering, Shandong University, Jinan 250061, China

² Engineering Research Center of Intelligent Unmanned System, Ministry of Education, Jinan 250061, China

on the product of exponential (POE) theory, and the results showed the effectiveness and precision of the integrated model. Chen et al. [5] developed an error model for a four-axis machine tool, in which the geometric errors of axis were regarded as a differential motion, and a Spearman rank correlation method was proposed to identify the key geometric error parameters which have a large effect on the tool posture of machine tools. E. Díaz-Tena et al. [6] proposed a methodology for evaluating the geometrical accuracy of a multi-axis machine based on Denavit and Hartenberg (D-H) method, in which the geometric errors were introduced as additional geometric parameters in each elemental transformation matrix. Zhang et al. [7] focused on system reliability and global sensitivity analyses of machine tools through the multiplicative dimensional reduction method (M-DRM), but the results were only verified in the three-axis vertical milling machine tool by Monte Carlo simulation method. Cheng [8] employed multi-body theory to establish a geometric error model of a 3-axis machine tool and identified the key geometric error elements by Sobol sensitivity analysis method. Cheng et al. [9] proposed a method based on the product of exponential screw theory to obtain the error model of a five-axis machine tool, then identified the key geometric errors, which have a greater influence on the machining accuracy, by global sensitivity analysis based on Morris method. Hong et al. [10] focused on the error motions of rotary axes on a five-axis machine tool and discussed the influence of position-dependent geometric errors of rotary axes on the machining accuracy of cone frustum machined. Lin and Lee proposed a systematically mathematical analysis method to analyze the assembly error of five-axis machine tools based on form-shaping theory [11]. Fu et al. [12] developed an integrated geometric error model of a machine tool based on the differential motion matrix, and the influences of geometric errors on the accuracy of the tool were calculated with the error vector of each axis.

The geometric error model of multi-axis machine tools is carried out by researchers mainly based on the D-H method [13, 14], or rigid body kinematics method with different theories [4, 5, 9]. However, Tang et al. [15] proposed a geometric error modeling method for a multi-axis system based on the stream of variation (SOV) theory, in which the axis was treated as a continuous workstation and the intermediate deviations were evaluated station by station. Nonetheless, previous studies mainly focused on conventional machine tools, in which multi-axis welding equipment is less mentioned, especially a kind of 6-axis welding equipment, consisting of a five-axis industry robot and a positioner, which is used in the field of intersecting pipes welding [16]. Compare with conventional machine

tools for turning, milling, boring, and grinding, the main geometric error sources of the welding equipment are kinematic errors and control errors. The geometric error sensitivity analysis of machine tools is commonly carried out with probabilistic analyses (e.g., [7, 8, 24]) or direct analyses (e.g., [14, 17, 20]). However, the insufficiency of these studies is that the geometric error model of machine tools is an approximate model. In this paper, a new method is proposed to analyze the geometric error of multi-axis machine based on Lie theory, which considers the orientation and position deviation of the welding torch at the same time.

The rest of the paper is organized as follows: Section 2 introduces the kinematics of rigid body motion, including Lie group and Lie algebra theory to describe rigid motion. In Section 3, the geometric errors of the 6-axis welding equipment are analyzed, and the geometric error model of the 6-axis welding equipment is established based on Lie theory. In Section 4, a new method is proposed to evaluate the influence of geometric errors by treating the deviation of the welding torch as a distance metrics in $SE(3)$, and a new sensitivity coefficient for geometric errors is proposed by considering the reality. The numerical simulations and discussion are carried out in Section 5. Conclusions are given in Section 6.

2 Kinematics of rigid body motion based on Lie theory

The rigid body motion like machine tools or manipulators can be described by a curve in the group of rigid motions in three-dimensional Euclidean space. In mathematical discussion of machine tools or manipulators, the Lie group $SE(3)$ is bound to play a fundamental role. The element $g \in SE(3)$ can be regarded as a mapping transformation $g : \mathbb{R}^3 \rightarrow \mathbb{R}^3$ in the form of $g(x) = Rx + p$, showing the distance and posture between points [22]. In general, the homogeneous $g \in SE(3)$ can be written as:

$$g = \begin{bmatrix} R & p \\ 0 & 1 \end{bmatrix} \quad (1)$$

where $R \in SO(3)$ represents the rotation matrix in \mathbb{R}^3 , $p \in \mathbb{R}^3$ is the translation vector, $SO(3) = \{R \in \mathbb{R}^{3 \times 3} : RR^T = I, \det R = 1\}$ represents the rotation group of \mathbb{R}^3 .

The Lie algebra of $g \in SE(3)$ can be defined as $\hat{\xi} \in se(3)$, and $\hat{\xi}$ also known as a twist. The matrix form of $\hat{\xi}$ can be expressed as:

$$\hat{\xi} = \begin{bmatrix} \hat{\omega} & v \\ 0 & 0 \end{bmatrix} \quad (2)$$

where $\omega \in \mathbb{R}^3$ and $v \in \mathbb{R}^3$, $\hat{\omega} \in so(3)$ is a 3×3 skew symmetric matrix. $so(3)$ represents the Lie algebra of $SO(3)$, and if $\omega = [\omega_x \ \omega_y \ \omega_z]^T$, $\hat{\omega}$ can be written as:

$$\hat{\omega} = \begin{bmatrix} 0 & -\omega_z & \omega_y \\ \omega_z & 0 & -\omega_x \\ -\omega_y & \omega_x & 0 \end{bmatrix} \tag{3}$$

The exponential map can be used to map $\hat{\xi} \in se(3)$ into the group $g \in SE(3)$, which means, one can obtain:

$$g = \exp(\hat{\xi}\theta) = \begin{bmatrix} R & p \\ 0 & 1 \end{bmatrix} \tag{4}$$

when $\omega = 0$, $\hat{\xi} = \begin{bmatrix} 0 & v \\ 0 & 0 \end{bmatrix}$, it represents pure translational motion of rigid body, then

$$g = e^{\hat{\xi}\theta} = \begin{bmatrix} I & v\theta \\ 0 & 1 \end{bmatrix} \tag{5}$$

when $v = 0$, $\hat{\xi} = \begin{bmatrix} \hat{\omega} & 0 \\ 0 & 0 \end{bmatrix}$, it represents pure rotational motion of rigid body, then

$$g = e^{\hat{\xi}\theta} = \begin{bmatrix} e^{\hat{\omega}\theta} & 0 \\ 0 & 1 \end{bmatrix} \tag{6}$$

when $\omega \neq 0$ and $\|\omega\| = 1$,

$$g = e^{\hat{\xi}\theta} = \begin{bmatrix} e^{\hat{\omega}\theta} & (I - e^{\hat{\omega}\theta})\omega \times v + \omega\omega^T v\theta \\ 0 & 1 \end{bmatrix} \tag{7}$$

The rotational part $e^{\hat{\omega}\theta}$ in Taylor series expansions can be transformed by the means of triangular progression, then

$$R = e^{\hat{\omega}\theta} = I + \hat{\omega}\sin\theta + \hat{\omega}^2(1 - \cos\theta) \tag{8}$$

The mapping $\hat{\xi} \in se(3) \mapsto \xi = (v^T, \omega^T)^T \in \mathbb{R}^6$ is isomorphic, where ξ is known as the ray coordinate or twist coordinate of $\hat{\xi}$. In 3-dimensional Euclidean space, the final transformation matrix of the rigid body moves from point a to point b can be expressed as:

$$g_{ab}(\theta) = e^{\hat{\xi}\theta} g_{ab}(0) \tag{9}$$

where $g_{ab}(0)$ represents the initial transformation matrix, $\hat{\xi}$ represents the unit twist of the motion from a to b , $\theta \in \mathbb{R}$ represents the rotation angle from a to b when $\omega \neq 0$, or the distance from a to b when $\omega = 0$.

Considering $g_{ab}(0) \in SE(3)$ and $g_{ab}(\theta) \in SE(3)$, the Lie algebra of $g_{ab}(0)$ and $g_{ab}(\theta)$ can be defined as $\hat{\xi}_{ab}$ and $\hat{\xi}'_{ab}$, respectively. Thus, Eq. 9 can be rewritten as:

$$\hat{\xi}'_{ab} = Ad(e^{\hat{\xi}\theta})\hat{\xi}_{ab} \tag{10}$$

where $Ad(e^{\hat{\xi}\theta})$ is the adjoint transformation associated with $e^{\hat{\xi}\theta}$.

Given $g = e^{\hat{\xi}\theta} = \begin{bmatrix} R & p \\ 0 & 1 \end{bmatrix}$, the adjoint matrix of g is given as

$$Ad(g) = Ad(e^{\hat{\xi}\theta}) = \begin{bmatrix} R & \hat{p}R \\ 0 & R \end{bmatrix} \tag{11}$$

For an n degree of freedom (DOF) open-chain manipulator, the forward kinematics can be expressed as:

$$g_{ST}(\theta_1, \theta_2, \dots, \theta_n) = e^{\hat{\xi}_1\theta_1} e^{\hat{\xi}_2\theta_2} \dots e^{\hat{\xi}_n\theta_n} g_{ST}(0) \tag{12}$$

where $g_{ST}(0)$ represents the initial transformation matrix, $\theta_1, \theta_2, \dots, \theta_n$ represent the joint angle variable or prismatic joint variable of link 1, link 2, ..., link n , respectively.

3 Geometric error modeling of the 6-axis welding equipment

The 6-axis welding equipment is based on a common main pipe and consists of a chain robot and positioner, which is different from the conventional welding equipment. The chain robot has five DOF, including three translational axes, i.e., X-axis, Y-axis, and Z-axis, and two postural axes, U-axis and V-axis, respectively. The U-axis rotates around X-axis, and V-axis rotates around Y-axis. The one DOF positioner, B-axis, is used to rotate the main pipe, which rotates around Y-axis. The kinematics of the 6-axis welding equipment is shown in Fig. 1, and the reference coordinate system (RCS) is set at the center axis of the main pipe, which is coincident with the User Coordinate System defined in [16]. The welding torch coordinate system (TCS) is coincident with the RCS in the origin. With different tools, the 6-axis welding equipment can not only finish welding but also cut the intersection curve for pipes.

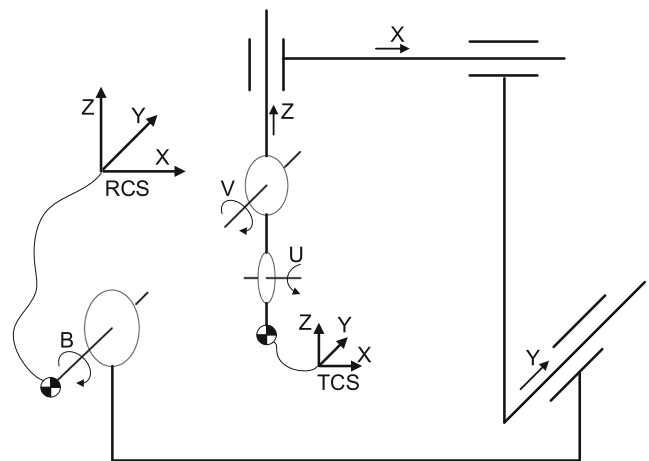


Fig. 1 The kinematics of the 6-axis welding equipment

3.1 Geometric error modeling of axis

In general, the position and posture of a rigid body in 3-dimensional space can be described by 3 location parameters and 3 orientation parameters. Similarly, there are six error components for a translational axis: the positioning error, two straightness error motions, roll error motion, and two tilt error motions, which are called pitch and yaw error motion for horizontal axis [2]. For the 6-axis welding equipment, there are 3 translational axes and 3 rotation axes, and the kinematics model of each axis can be described by the Lie group.

Usually, when the six error components of X-axis are ignored, the ideal kinematics model of X-axis can be written as:

$$g_x(x) = e^{\hat{\xi}_x x} g_x(0) \tag{13}$$

where $\xi_x = (1, 0, 0, 0, 0, 0)^T$ is the unit twist coordinate of X-axis, $g_x(0)$ is the initial transformation matrix, and x is the amount of translation that moves along X-axis.

However, the actual kinematics model of X-axis is influenced by various reasons. Geometric error components exist in each axis. As shown in Fig. 2, the six error components of X-axis, $\delta_x(x)$ represents the linear error, $\delta_y(x)$ and $\delta_z(x)$ represent the straightness error in Y-axis and Z-axis direction, $\epsilon_x(x)$ represents the roll error, and $\epsilon_y(x)$ and $\epsilon_z(x)$ represent the tilt error around Y-axis and Z-axis, respectively. When the geometric errors of X-axis are treated as the twist motion. According to [23], the actual kinematics model of X-axis can be written as:

$$g_x(x) = e^{\hat{\xi}_x x} e^{\hat{\xi}_y \delta_y(x)} e^{\hat{\xi}_z \delta_z(x)} e^{\hat{\xi}_a \epsilon_x(x)} e^{\hat{\xi}_b \epsilon_y(x)} e^{\hat{\xi}_c \epsilon_z(x)} g_x(0) \tag{14}$$

where $\xi_y = (0, 1, 0, 0, 0, 0)^T$ and $\xi_z = (0, 0, 1, 0, 0, 0)^T$ are the unit twist coordinate of Y-axis and Z-axis, respectively. $\xi_b = (0, 0, 0, 0, 1, 0)^T$ is the unit twist

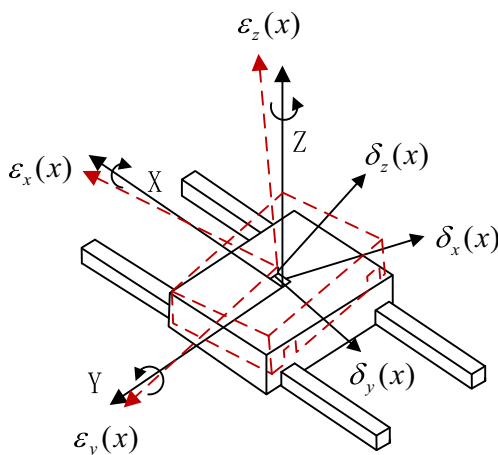


Fig. 2 Error components of X axis

coordinate of B-axis; $\xi_a = (0, 0, 0, 1, 0, 0)^T$ is the unit twist coordinate of A-axis, which rotates around X-axis; $\xi_c = (0, 0, 0, 0, 0, 1)^T$ is the unit twist coordinate of C-axis, which rotates around Z-axis. On account of its complication, the actual transformation matrix of X-axis is not formulated in detail here.

The actual kinematics model of X-axis can be regarded as two parts. One is the ideal translation along X-axis, and the other is the pose deviation caused by the geometric errors which can be regarded as a smooth motion in \mathbb{R}^3 . Thus, Eq. 14 can be rewritten as:

$$g_x(x) = e^{\hat{\xi}_x x} e^{\hat{\xi}_{xe}} g_x(0) \tag{15}$$

where $e^{\hat{\xi}_{xe}}$ represents the transformation matrix of error part and ξ_{xe} represents the equivalent twist coordinate of the pose deviation of X-axis.

For the rotation axis, as shown in Fig. 3, the six error components of the B-axis. $\delta_y(b)$ represents the axial error of B-axis, and $\delta_x(b)$ and $\delta_z(b)$ represent the radial error of B-axis in X direction and Z direction, respectively. $\epsilon_y(b)$ represents the angular positioning error, and $\epsilon_x(b)$ and $\epsilon_z(b)$ represent the tilt error around X-axis and Z-axis, respectively. The ideal kinematics of the B-axis can be written as:

$$g_b(b) = e^{\hat{\xi}_b b} g_b(0) \tag{16}$$

In the same way, when considering the geometric errors of the B-axis, the actual kinematics model of B-axis can be written as:

$$g_b(b) = e^{\hat{\xi}_b b} e^{\hat{\xi}_{be}} g_b(0) \tag{17}$$

where $e^{\hat{\xi}_{be}}$ represents the transformation matrix of error part and ξ_{be} represents the equivalent twist coordinate of the pose deviation of B-axis.

For the 6-axis welding equipment, there are 36 geometric error components, which are shown in Table 1. δ_x , δ_y , and δ_z represent the location error components, where the

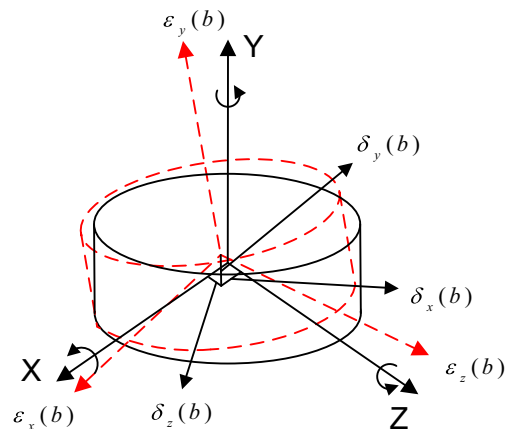


Fig. 3 Error components of B-axis

Table 1 Geometric errors of the 6-axis welding equipment

Sequence number	Axis	Error components
1 – 6	B	$\delta_x(b), \delta_y(b), \delta_z(b), \epsilon_x(b), \epsilon_y(b), \epsilon_z(b)$
7 – 12	U	$\delta_x(u), \delta_y(u), \delta_z(u), \epsilon_x(u), \epsilon_y(u), \epsilon_z(u)$
13 – 18	V	$\delta_x(v), \delta_y(v), \delta_z(v), \epsilon_x(v), \epsilon_y(v), \epsilon_z(v)$
19 – 24	X	$\delta_x(x), \delta_y(x), \delta_z(x), \epsilon_x(x), \epsilon_y(x), \epsilon_z(x)$
25 – 30	Y	$\delta_x(y), \delta_y(y), \delta_z(y), \epsilon_x(y), \epsilon_y(y), \epsilon_z(y)$
31 – 36	Z	$\delta_x(z), \delta_y(z), \delta_z(z), \epsilon_x(z), \epsilon_y(z), \epsilon_z(z)$

subscript represents the error direction; $\epsilon_x, \epsilon_y,$ and ϵ_z represent the angular error components, where the subscript represents the rotation axis of error; $b, u,$ and v are the rotation angle of B-axis, U-axis, and V-axis, respectively; $x, y,$ and z are the translational distances of X-axis, Y-axis, and Z-axis, respectively.

3.2 Geometric error modeling of the 6-axis welding equipment

The topological structure of the 6-axis welding equipment is shown in Fig. 4. The equipment can be considered as an open kinematic chain from the working table to the welding torch, and the machine bed can be ignored due to the twist of the machine bed is zero. Then, the order of the kinematics model is shown as $B \rightarrow Y \rightarrow X \rightarrow Z \rightarrow V \rightarrow U$. According to Section 2, the ideal kinematics model of the 6-axis welding equipment can be obtained as:

$$g_i = e^{\hat{\xi}_b b} e^{\hat{\xi}_y y} e^{\hat{\xi}_x x} e^{\hat{\xi}_z z} e^{\hat{\xi}_v v} e^{\hat{\xi}_u u} g(0) \tag{18}$$

where $\xi_u = (0, 0, l_1, 1, 0, 0)^T$ and $\xi_v = (0, 0, l_1 + l_2, 0, 1, 0)^T$ are unit twist coordinates of U-axis and V-axis, respectively; l_1 represents the distance from the welding torch tip to the center of U-axis, l_2 represents the distance from the center of U-axis to the center of V-axis, and $g(0) = I_{4 \times 4}$ is the initial transformational matrix.

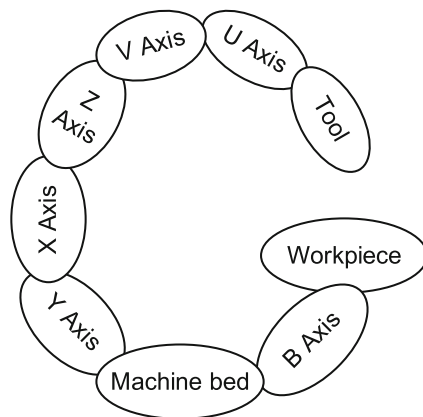


Fig. 4 Topological structure of the 6-axis welding equipment

However, the existence of geometric errors in each axis, affecting the accuracy of the equipment, is inevitable. When the geometric errors are taken into account, the actual kinematics model of the 6-axis automatic welding equipment can be expressed as:

$$g_r = e^{\hat{\xi}_b b} e^{\hat{\xi}_{be}} e^{\hat{\xi}_y y} e^{\hat{\xi}_{ye}} e^{\hat{\xi}_x x} e^{\hat{\xi}_{xe}} e^{\hat{\xi}_z z} e^{\hat{\xi}_{ze}} e^{\hat{\xi}_v v} e^{\hat{\xi}_{ve}} e^{\hat{\xi}_u u} e^{\hat{\xi}_{ue}} g(0) \tag{19}$$

where $\hat{\xi}_{ye}, \hat{\xi}_{ze}, \hat{\xi}_{ve},$ and $\hat{\xi}_{ue}$ are the equivalent twist of the geometric errors existing in Y-axis, Z-axis, V-axis, and U-axis, respectively.

The difference between the ideal and actual homogeneous coordinates of the welding torch tip is the pose error of the welding torch, which can be defined as g_e , then

$$g_r = g_i * g_e \tag{20}$$

Thus, the geometric error model of the 6-axis welding equipment can be expressed as:

$$g_e = g_i^{-1} * g_r = \begin{bmatrix} R_e & p_e \\ 0 & 1 \end{bmatrix} \tag{21}$$

where p_e represents the position error of the welding torch, and R_e represents the orientation error of the welding torch. On account of its complication, the actual transformation matrix is also not formulated in detail here.

4 Sensitivity analysis based on Lie theory

According to the geometric error model, the deviation of the welding torch pose can be influenced by 36 geometric error components. Among these, some geometric errors have a significant impact on the accuracy of the welding equipment, and some geometric errors have less impact on the accuracy of the welding equipment. However, it is really difficult to measure each geometric error and compensate for all geometric errors. To improve the accuracy of a machine tool, the essential geometric error components that affect the accuracy of the tool should be identified first. Therefore, the sensitivity analysis of geometric errors is fundamentally essential.

4.1 Evaluation for the influence of geometric errors

As shown in Fig. 5, the deviation of the welding torch, introduced by the geometric errors, can be regarded as a smooth motion of the welding torch tip moving from the actual pose to the ideal pose. Thus, the impact of geometric errors on the accuracy of the welding torch can be regarded as the impact of geometric errors on the smooth motion from the actual pose to the ideal pose. Since no natural length scale exists for physical space, the effect of geometrical errors on the welding equipment is complex. However,

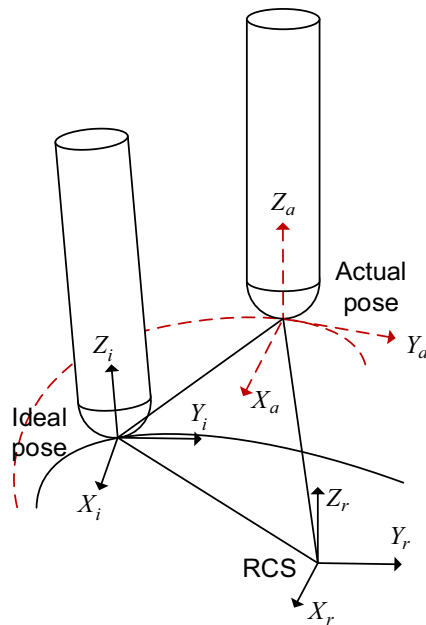


Fig. 5 Deviation of the welding torch

according to [18, 19], the distance metrics of the tool frame and desired goal frame can be constructed in SE(3) under the left or right translations. On this basis, the distance metrics from g_i to $g_r = g_i * g_e$ can be calculated. And, according to the geometric error model, the left invariant distance metric is suitable for analyzing the sensitivity of geometric errors. This distance metric of left translations can be defined as:

$$d(g_1, g_2) = \sqrt{c \left\| \log(R_1^{-1} R_2) \right\|^2 + d \|p_2 - p_1\|^2}$$

where g_1 and g_2 are elements of $SE(3)$, $\|\cdot\|$ denotes the Euclidean norm, and c and d are scale factors to balance the position component and orientation component.

Hence, the influence of geometric errors can be evaluated by the distance metrics from the ideal pose to the actual pose, and the distance metrics can be written as:

$$d(g_i, g_r) = d(g_i * g_0, g_i * g_e) = d(g_0, g_e) \tag{22}$$

$$= \sqrt{c \left\| \log R_e \right\|^2 + d \|p_e\|^2}$$

For the 6-axis welding equipment, the deviation between the ideal welding trajectory and the actual welding trajectory can be calculated by Eq. 22. Thus, for a complete machining path, the root mean square error introduced by geometric errors can be obtained as:

$$RMSE = \sqrt{\frac{1}{m} \sum_{i=1}^m d(g_0, g_e)^2} \tag{23}$$

where m represents the sample number of the machining path.

4.2 Sensitivity coefficient of the geometric error

To evaluate the influence of geometric errors on the accuracy of a machine tool, the sensitivity coefficient of geometric error is often employed. In general, the sensitivity coefficient of geometric error can be obtained by probabilistic analyses or direct analyses. For the probabilistic analysis method, the distribution of geometric error components is required, which can be obtained by corresponding measure methods like [8, 24], or assumed like [7]. However, the distribution of geometric error components in each axis is uncertain, especially the rotation axis. The differential method is used to obtain the sensitivity indices in the direct analysis, and the results are generally good. However, to simplify the calculation, the geometric error model of machine tools is an approximate treatment in most studies. To identify the dominant geometric error, considering the application of the 6-axis welding machine, the geometric error components set as a constant are desirable for sensitivity analysis.

The geometric error components of each axis set or separately set as a constant are a common approach applied in the geometric error sensitivity analysis of the multi-axis machine tools [14, 15, 17, 21]. Nevertheless, it is inevitable that the geometric errors of the machine tool exist and affect the tool pose in actual situations, even after the compensation. It is insufficient to consider the geometric error components separately or just set the geometric error as a constant. Therefore, considering the actual state of geometric errors, the basic value of each geometric error should be defined at first, and the accuracy of the tool pose affected by the increment of geometric error evaluated. In other words, the geometric error, which has the best improvement on the accuracy of the machine tool after compensation, is the key geometric error of the machine tool.

For the difference of units, the basic value is different for position error and angular error. The 36 geometric errors of the 6-axis welding equipment can be divided into positional error and angular error. Hence, we define Δ_p and Δ_a to represent the fundamental value of positional error and angular error, respectively. The basic root mean square error is denoted by:

$$E_0 = \sqrt{\frac{1}{m} \sum_{i=1}^m d_e^2} \tag{24}$$

where d_e is the basic distance metrics between the ideal tool pose to the actual tool pose when geometric errors are taken the basic value.

To figure out the influence of each geometric error, the geometric error plus an increment value systematically at the basic value of Δ_p or Δ_a . Thus, for the 36 geometric

errors of the 6-axis welding equipment, the root mean square error can be expressed as follows:

$$E_j = \sqrt{\frac{1}{m} \sum_{i=1}^m d'^2_{ei}} \tag{25}$$

where j is the sequence number, represents the geometric error component related to Table 1; d'_e is the distance metrics between the ideal tool pose to the actual tool pose when the geometric error j plus the increment value and the others are set at the basic value.

The impact on the tool tip of geometric errors is different: each geometric error has a positive or negative effect on the welding torch pose. The improvement of the accuracy of the welding torch can be evaluated by the comparison of the mean square errors. Therefore, the value between E_j and E_0 can be regarded as the size of effect introduced by the increment value of geometric error, which can be denoted as:

$$K_j = |E_j - E_0| \tag{26}$$

The new sensitivity coefficients, for the 36 geometric errors of the 6-axis welding equipment, can be defined as:

$$S_j = K_j / \sum_{i=1}^{36} K_i \tag{27}$$

5 Numerical results and discussion

In this section, the numerical simulations are carried out to verify the effectiveness of the geometric error model and sensitivity analysis of all axes. The welding trajectory planning for intersecting pipes introduced in literature [16] is a typical algorithm to weld intersecting pipes, which can be used to verify the kinematics model and conduct the sensitivity analysis of geometric errors.

5.1 Parameters for numerical simulation

For computational expediency, the parameters of welding equipment are set at $l_1 = 400$ mm, and $l_2 = 150$ mm. Thus, the corresponding unit twist coordinates of the U-axis and V-axis are $\xi_u = (0, 0, 400, 1, 0, 0)^T$ and $\xi_v = (0, 0, 550, 0, 1, 0)^T$, respectively. The basic parameters and welding technological requirements for two intersecting pipes are obtained from the literature [25], which are shown in Table 2. And, the welding torch trajectory planning without swing motion. As shown in Fig. 6, the ideal welding trajectory for intersecting pipes is obtained by the kinematics model of the 6-welding equipment based on Lie theory.

To closely resemble reality, the influence of basic geometric errors is taken into consideration by setting the

Table 2 The welding parameters for intersecting pipes

Parameter name	Value
Main pipe diameter	220mm
Branch pipe diameter	140mm
Offset distance	0mm
Crossing angle	$\pi/2$
Travel angle	0
Working angle	0

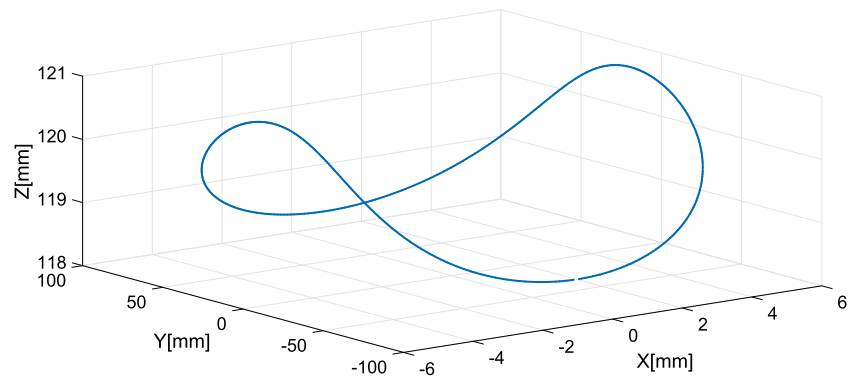
basic value of geometric errors. Alternatively, the basic position errors are set at $\Delta_p = 1$ μ m, and the basic angular errors are set at $\Delta_a = 10$ μ rad. As the pose error of welding torch can be divided into the position error and orientation error, the scale factors c and d , mentioned in Section 4.1, become particularly important. For different application scenarios, the scale factors can be selected independently based on the weight of position and orientation. Here, c and d are taken at the same value (where $c = d = 1$).

To investigate the error contribution of each error, the geometric error components of each axis are sequential plus the corresponding increment on the basic value. Above the basal value of Δ_p and Δ_a , the increment value of position error is set at 1 μ m, and the increment value of angular error set at 10 μ rad. Then, the deviation of the welding torch pose introduced by the geometric errors can be obtained by Eq. 25, and the sensitivity coefficient of each geometric error can be obtained according to Eq. 27. In numerical simulations, the sample number m is set at 500.

5.2 Simulation results and discussion

Shown in Fig. 7 are the numerical simulation result of sensitivity coefficient for each geometric error. The sensitivity coefficients range from 0.0003 to 0.1515, where the angular error $\epsilon_z(u)$ has a minimal impact and $\epsilon_y(z)$ has a maximum impact on the accuracy of the welding torch. For the 6-axis welding equipment, the angular errors $\epsilon_y(x)$, $\epsilon_z(x)$, $\epsilon_y(z)$, and $\epsilon_z(z)$ have a stronger influence on the welding torch pose compared with other geometric errors, which means that the angular errors $\epsilon_y(x)$, $\epsilon_z(x)$, $\epsilon_y(z)$, and $\epsilon_z(z)$ have priority when compensating the geometric errors. According to the difference of units, the sum of sensitivity coefficient of position error components is 0.36, and the sum of sensitivity coefficient of the angular error components is 0.64. However, it is easy to find the orientation error caused by angular errors and the deviation of spatial location caused by both position errors and angular errors in geometric error model. Compared with position error components, the angular errors have a greater impact on the deviation of the welding torch pose, and the sensitivity coefficients of the geometric errors $\epsilon_y(x)$, $\epsilon_z(x)$, $\epsilon_y(z)$, and $\epsilon_z(z)$ are larger

Fig. 6 Ideal welding trajectory for intersecting pipes



than the others, which means that more attention should be paid on the straightness of the X-axis and Z-axis.

When the position error and angular error analysis separated, the sensitivity coefficient of position error can be defined as:

$$S_{pj} = K_{pj} / \sum_{i=1}^{18} K_{pi} \tag{28}$$

where the subscript p represents the sensitivity coefficient of position error and the subscript j represents the sequence number of position error.

Similarity, the sensitivity coefficient of angular error can be defined as:

$$S_{aj} = K_{aj} / \sum_{i=1}^{18} K_{ai} \tag{29}$$

where the subscript a represents the sensitivity coefficient of angular error, and the subscript j represents the sequence number of angular error.

The sensitivity coefficients of position errors and angular errors are shown in Figs. 8 and 9, respectively. Besides the angular errors $\epsilon_y(x)$, $\epsilon_z(x)$, $\epsilon_y(z)$, and $\epsilon_z(z)$, the angular errors of B-axis have stronger influence on the accuracy of the welding torch. The angular errors of the U-axis and V-axis can be ignored when compared with the others, and the angular errors around Y-axis impact the welding torch pose most, followed by Z-axis. The position error components of B-axis, X-axis, Y-axis, and Z-axis have the same effect on the accuracy of the welding torch. The position error in the X direction impacts the welding torch most, followed by Z direction.

To further verify the sensitivity analysis method and figure out the effect of geometric errors, the distance metrics

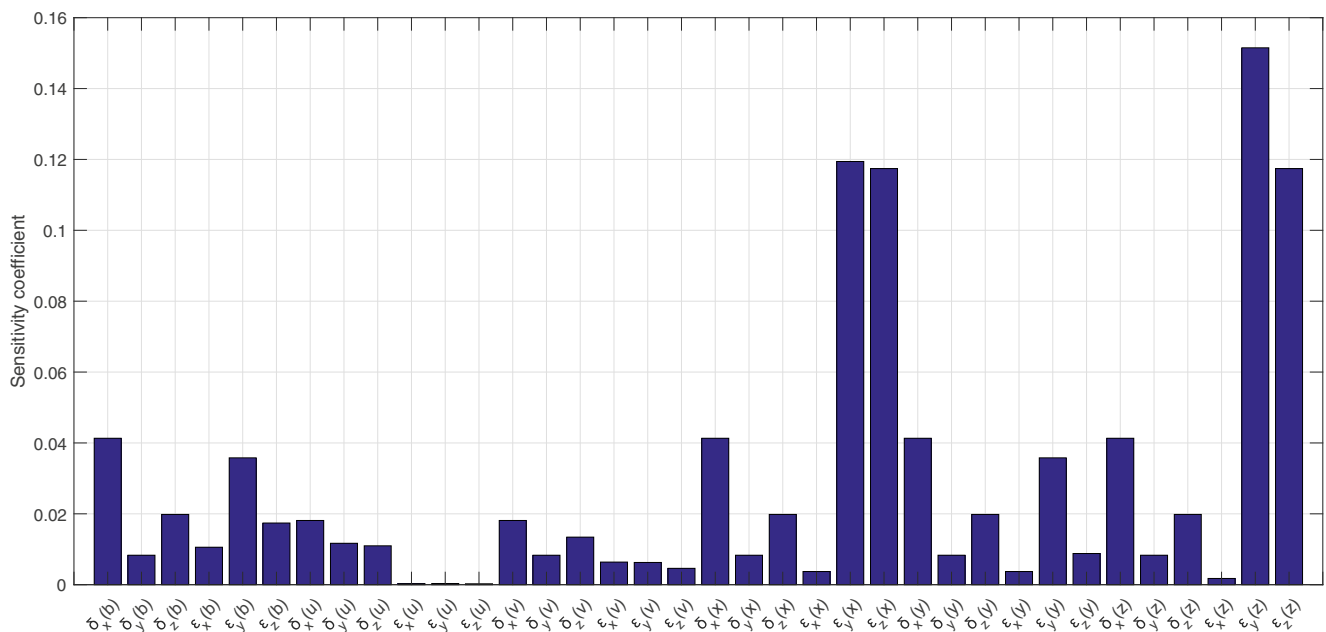


Fig. 7 Sensitivity coefficient of geometric error components

Fig. 8 Sensitivity coefficient of angular errors

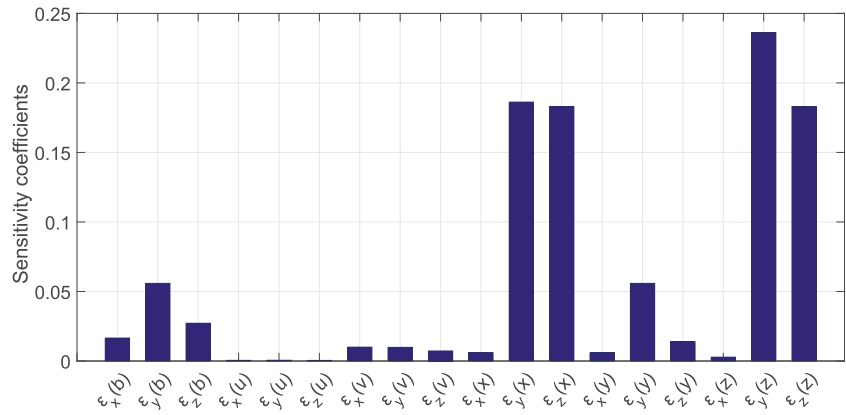


Fig. 9 Sensitivity coefficient of position errors

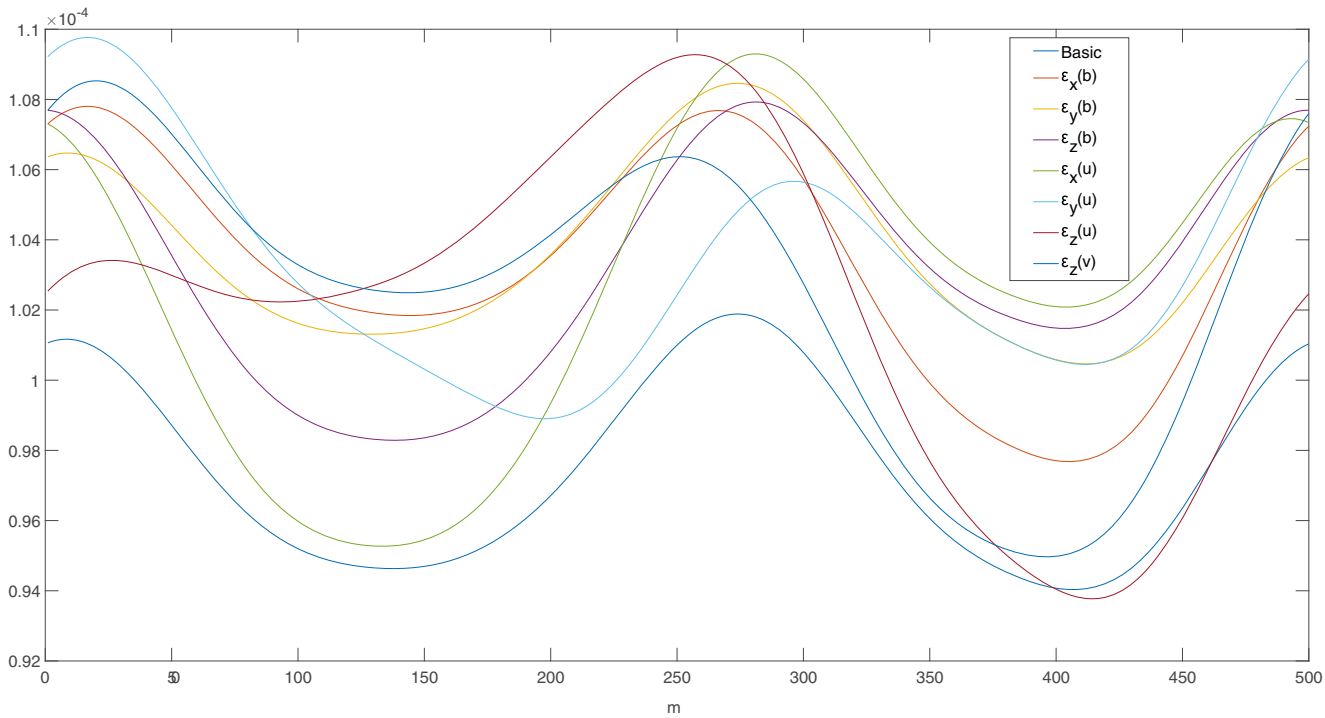
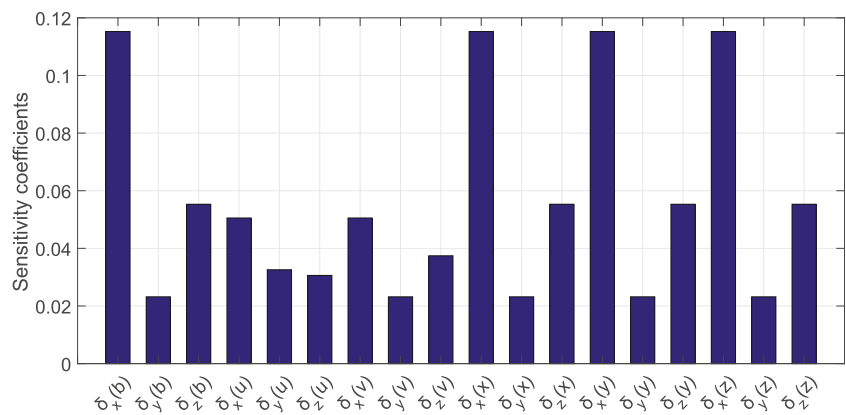


Fig. 10 The orientation deviation of the welding torch. The Basic represents the orientation deviation when the geometric errors are taken the basic value

$d(g_0, g_e)$ can be divided into 2 parts: $\log R_e$ represents the orientation deviation and p_e represents the position deviation of the welding torch. According to [18], $\log R_e = d(R_e, R_0)$, and the simulation result of the orientation deviation is shown in Fig. 10. For the angular errors of X, Y and Z axes have the same effect as B-axis, $\epsilon_y(v)$ same as $\epsilon_y(b)$, and $\epsilon_x(u)$ same as $\epsilon_x(v)$, on the orientation deviation of the welding torch, the angular error components of X-axis, Y-axis, Z-axis, $\epsilon_y(b)$, $\epsilon_x(v)$ are not shown in Fig. 10. The basic curve in Fig. 10 represents the orientation error distribution when the geometric errors are set at the basal value, and $\epsilon_x(b)$, $\epsilon_y(b)$, $\epsilon_z(b)$, $\epsilon_x(u)$, $\epsilon_y(u)$, $\epsilon_z(u)$, and $\epsilon_z(v)$ represent the orientation error distribution of the welding torch when the corresponding angular error component plus the increment value and the other geometric errors remain unchanged. And on the basis of all geometric errors set at

the basic value, when the angular errors are varied systematically, the changes of impact on the orientation accuracy of the welding torch are roughly similar. The position error distribution of the welding torch is shown in Fig. 11, when all geometric errors are varied systematically. The Basic curve represents the position error of the welding torch when the geometric errors are taken the basic value. It is obvious that $\epsilon_y(x)$, $\epsilon_z(x)$, $\epsilon_y(z)$, and $\epsilon_z(z)$ have a stronger influence on the position accuracy of the welding torch, which also verifies the validity of new sensitivity analysis method. It is evident from Figs. 10 and 11 that the posture error of the welding torch is relatively small compared to the position error of the welding torch, which means the distance metrics $d(g_0, g_e)$ is predominantly affected by the position error of the welding torch, and the angular errors of each axis have a greater impact on the accuracy of the welding torch.

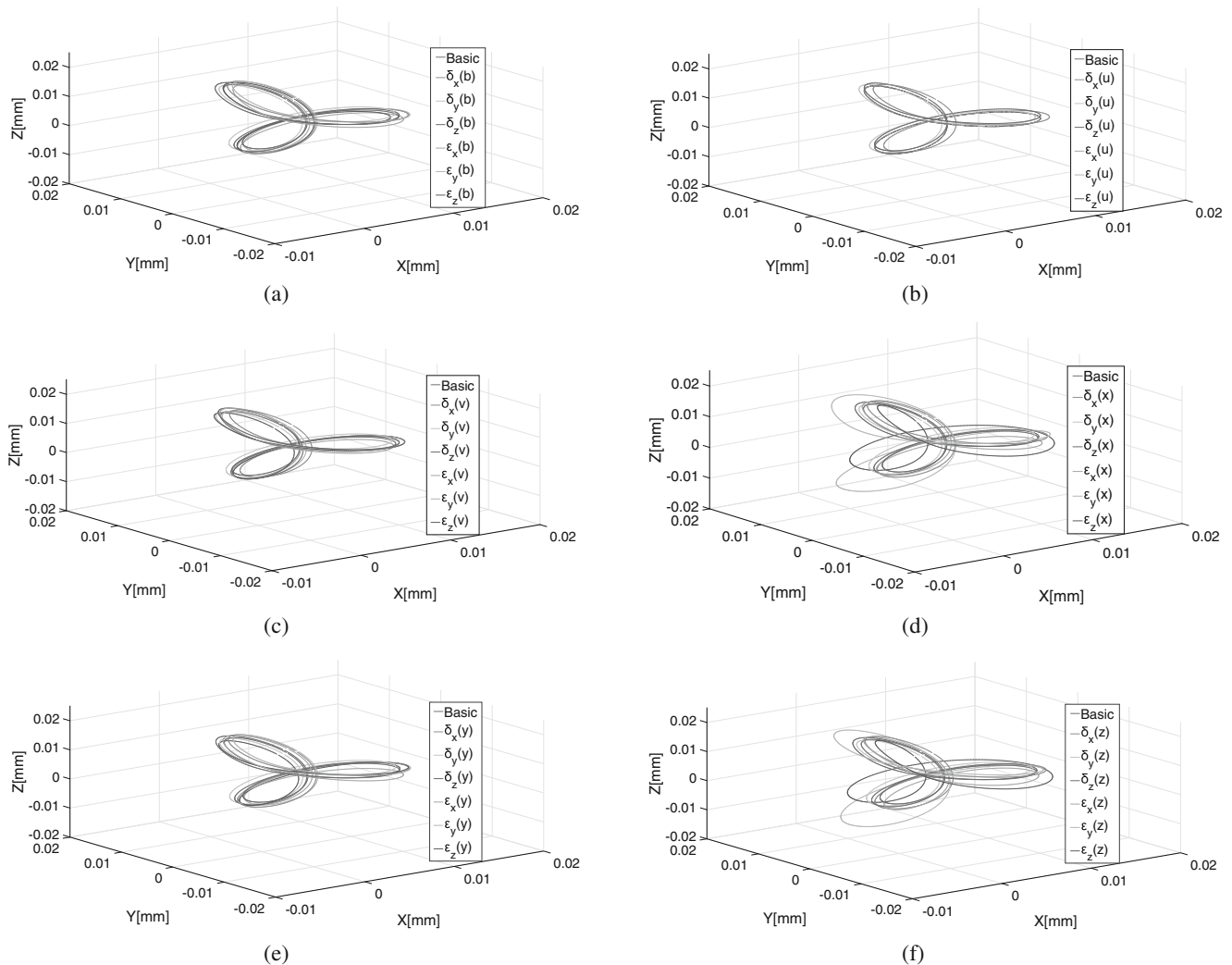


Fig. 11 The position deviation of the welding torch when the geometric errors are changed systematically. The Basic represents the position deviation when the geometric errors are taken the basic value. **a** B-axis,

b U-axis, **c** V-axis, **d** X-axis, **e** Y-axis, and **f** Z-axis are the position deviations of the welding torch when the geometric errors of each axis are changed systematically

6 Conclusion

In this paper, the geometric error modeling and its sensitivity analysis of a new automation welding equipment for intersecting pipes welding, consisting of a positioner and 5-axis industry robot, were studied. Compared with the traditional machine tool, the 6-axis welding equipment focuses on machining along the trajectory while the traditional machine tools focus on surface machining. The strict error model of the 6-axis welding equipment including 36 geometric errors was established based on the Lie theory without approximate treatment. Besides, a new sensitivity analysis method was proposed to find out the key geometric error components which have a stronger influence on the welding torch pose. The sensitivity coefficient of each geometric error component was obtained and the dominant geometric errors that affected the accuracy of the machine were identified by applying the new sensitivity analysis method. The major contributions of the paper are as follows:

- (1) The strict geometric error model of the 6-axis welding equipment is established, which contains 36 geometric error components, based on Lie theory.
- (2) A new sensitivity analysis method is proposed based on the distance metrics of SE(3), which considers the position and orientation error of the welding torch at the same time. The proposed method is more convenient and flexible, when compared with previous studies of the geometric error sensitivity analysis method.
- (3) To closely resemble reality, a new sensitivity coefficient of geometric error is proposed by considering the basic value of geometric error.
- (4) Numerical simulations are taken to verify the sensitivity analysis method, and the dominant geometric errors of the 6-axis welding equipment were identified, which lays the foundation for follow-up studies.

Author's contributions Weihua Fang was a major contributor in writing the manuscript. All authors read and approved the final manuscript.

Funding The authors received research funding by the National Key Research and Development Plan of China under Grant No.2017YFB13035 and the Shandong Provincial Key Research and Development Program (Major Scientific and Technological Innovation Project) under Grant No. 2019JZZY010441.

Compliance with ethical standards

Conflict of interest The authors declare that they have no conflict of interest.

References

1. Huang T, Li Y, Tang G, Li S, Zhao X, Xianping L (2002) Error modeling, sensitivity analysis and assembly process of a class of 3-DOF parallel kinematic machines with parallel-gram struts. *Sci China Ser E-Technol Sci* 45:467–476. <https://doi.org/10.1360/02ye9054>
2. Schwenke H, Knapp W, Haitjema H, Weckenmann A, Schmitt R, Delbressine F (2008) Geometric error measurement and compensation of machines-an update. *CIRP Ann-Manuf Technol* 57(2):660–675. <https://doi.org/10.1016/j.cirp.2008.09.008>
3. Lin Y, Shen Y (2003) Modelling of Five-Axis Machine Tool Metrology Models Using the Matrix Summation Approach. *Int J Adv Manuf Technol* 21:243–248. <https://doi.org/10.1007/s001700300028>
4. Fu G, Fu J, Xu Y, Chen Z (2014) Product of exponential model for geometric error integration of multi-axis machine tools. *Int J Adv Manuf Technol* 71:1653–1667. <https://doi.org/10.1007/s00170-013-5586-5>
5. Chen J-x, Lin S-w, Zhou X-l (2016) A comprehensive error analysis method for the geometric error of multi-axis machine tool. *Int Mach Tools Manuf* 106:56–66. <https://doi.org/10.1016/j.ijmactools.2016.04.001>
6. Díaz-Tena E, Ugalde U, De Lacalle LL, De la Iglesia A, Calleja A, Campa FJ (2013) Propagation of assembly errors in multitasking machines by the homogenous matrix method. *Int J Adv Manuf Technol* 68:149–164. <https://doi.org/10.1007/s00170-012-4715-x>
7. Zhang X, Zhang Y, Pandey MD (2015) Global sensitivity analysis of a CNC machine tool: application of MDRM. *Int J Adv Manuf Technol* 81:159–169. <https://doi.org/10.1007/s00170-015-7128-9>
8. Cheng Q, Zhao H, Zhang G, Gu P, Cai L (2014) An analytical approach for crucial geometric errors identification of multi-axis machine tool based on global sensitivity analysis. *Int J Adv Manuf Technol* 75:107–121. <https://doi.org/10.1007/s00170-014-6133-8>
9. Cheng Q, Feng Q, Liu Z, Gu P, Zhang G (2016) Sensitivity analysis of machining accuracy of multi-axis machine tool based on POE screw theory and Morris method. *Int J Adv Manuf Technol* 84:2301–2318. <https://doi.org/10.1007/s00170-015-7791-x>
10. Hong C, Ibaraki S, Matsubara A (2011) Influence of position-dependent geometric errors of rotary axes on a machining test of cone frustum by five-axis machine tools. *Precis Eng* 35(1):1–11. <https://doi.org/10.1016/j.precisioneng.2010.09.004>
11. Lee RS, Lin YH (2012) Applying bidirectional kinematics to assembly error analysis for five-axis machine tools with general orthogonal configuration. *Int J Adv Manuf Technol* 62:1261–1272. <https://doi.org/10.1007/s00170-011-3860-y>
12. Fu G, Fu J, Xu Y, Chen Z, Lai J (2015) Accuracy enhancement of five-axis machine tool based on differential motion matrix: Geometric error modeling, identification and compensation. *Int J Mach Tools Manuf* 89:170–181. <https://doi.org/10.1016/j.ijmactools.2014.11.005>
13. Khan AW, Wuyi C (2010) Systematic geometric error modeling for workspace volumetric calibration of a 5-axis turbine blade grinding machine. *Chin J Aeronaut* 23(5):604–615. [https://doi.org/10.1016/S1000-9361\(09\)60261-2](https://doi.org/10.1016/S1000-9361(09)60261-2)
14. Chen G, Liang Y, Sun Y, Chen W, Wang B (2013) Volumetric error modeling and sensitivity analysis for designing a five-axis ultra-precision machine tool. *Int J Adv Manuf Technol* 68:2525–2534. <https://doi.org/10.1007/s00170-013-4874-4>
15. Tang H, Duan J-a, Lan S, Shui H (2015) A new geometric error modeling approach for multi-axis system based on stream of variation theory. *Int J Mach Tools Manuf* 92: 41–51. <https://doi.org/10.1016/j.ijmactools.2015.02.012>

16. Shi L, Tian X, Zhang C (2015) Automatic programming for industrial robot to weld intersecting pipes. *Int J Adv Manuf Technol* 81:2099–2107. <https://doi.org/10.1007/s00170-015-7331-8>
17. Li Q, Wang W, Jiang Y, Li H, Zhang J, Jiang Z (2018) A sensitivity method to analyze the volumetric error of five-axis machine tool. *Int J Adv Manuf Technol* 98:1791–1805. <https://doi.org/10.1007/s00170-018-2322-1>
18. Park FC (1995) Distance Metrics on the Rigid-Body Motions with Applications to Mechanism Design. *ASME J Mech Des* 117(1):48–54. <https://doi.org/10.1115/1.2826116>
19. Wang Y (2006) An incremental method for forward kinematics of parallel manipulators. In 2006 IEEE Conference on Robotics, Automation and Mechatronics, pp 1–5
20. Li J, Xie F, Liu X (2016) Geometric error modeling and sensitivity analysis of a five-axis machine tool. *Int J Adv Manuf Technol* 82:2037–2051. <https://doi.org/10.1007/s00170-015-7492-5>
21. Fu G, Gong H, Fu J, Gao H, Deng X (2019) Geometric error contribution modeling and sensitivity evaluating for each axis of five-axis machine tools based on POE theory and transforming differential changes between coordinate frames. *Int J Mach Tools Manuf* 147. <https://doi.org/10.1016/j.ijmactools.2019.103455>
22. Murray RM, Li Z, Sastry SS (1994) A mathematical introduction to robotic manipulation. CRC press, Boca Raton
23. Craig JJ (2009) Introduction to robotics: mechanics and control, 3/E. Pearson Education India
24. Guo S, Zhang D, Xi Y (2016) Global Quantitative Sensitivity Analysis and Compensation of Geometric Errors of CNC Machine Tool. *Math Probl Eng* 2016. <https://doi.org/10.1155/2016/2834718>
25. Shi L, Tian X (2015) Automation of main pipe-rotating welding scheme for intersecting pipes. *Int J Adv Manuf Technol* 77:955–964. <https://doi.org/10.1007/s00170-014-6526-8>

Publisher's note Springer Nature remains neutral with regard to jurisdictional claims in published maps and institutional affiliations.